



Enhanced oxygen diffusion in nano-structured ceria

Yu. I. Boyko¹ · V. I. Biletskyi¹ · V. V. Bogdanov¹ · R. V. Vovk¹ · G. Ya. Khadzhai¹ · I. L. Goulatis¹ · A. Chroneos^{2,3}

Received: 30 October 2017 / Accepted: 15 December 2017 / Published online: 15 January 2018
© The Author(s) 2018. This article is an open access publication

Abstract

Nano-structured polycrystalline CeO₂ is proposed to be used as a candidate electrolyte material for solid oxide fuel cells (SOFC) operating at temperatures ≤ 600 °C. Here we show that in this material the diffusion activation energy of oxygen ions is 0.35 eV. The diffusion mechanism corresponds to the “single-file” diffusion mechanism, associated with the presence of one-dimensional channels in the anion sublattice of CeO₂. The small grain size of the material ≈ 10 nm, as well as its stoichiometric state (Ce₂O₃), minimize the contribution of the electronic and polaron components of the electrical conductivity of this material, which also contribute to the optimization of SOFC operation.

1 Introduction

SOFCs are characterized by increased energy efficiency (> 60%), simplicity of technical realization, and limited emissions during operation [1–10]. These constitute SOFC important for both stationary and mobile applications. The efficiency of SOFC is strongly dependent upon the diffusion of oxygen ions (O²⁻) in the electrolyte. Presently, the most widely used electrolyte is the ZrO₂ polycrystalline doped with oxides such as Y₂O₃ (to form YSZ). These dopants in an amount of ≈ 10 mol% are increasing the concentration of vacancies in the oxygen sublattice of the electrolyte material, which in turn facilitate oxygen ions diffusion. Additionally, yttria stabilizes the fluorite crystal structure of ZrO₂ from room temperature to 1000 °C [1].

The power of the SOFC source is determined by the flux J of O²⁻ ions diffusing through the electrolyte from the cathode to the anode at a partial oxygen pressure of ≈ 0.2 bar. The value of the oxygen ions flux J is proportional to the electrical conductivity coefficient of the electrolyte material σ , which in turn depends from the diffusion coefficient D_V and the temperature T :

$$J \sim \sigma \sim D_V \sim \exp(-Q/kT). \quad (1)$$

Here, D_V is the diffusion coefficient of oxygen ions O²⁻ in the electrolyte, Q is the activation energy of diffusion, and k is Boltzmann's constant. The really consumed power of SOFC using electrolyte YSZ (ZrO₂ + 8% Y₂O₃) is determined by the value of $\sigma \approx (10^{-3} - 10^{-1}) \Omega^{-1} \text{ cm}^{-1}$, which is achieved in the temperature range $T \approx 600 - 1000$ °C. The activation energy for YSZ is 0.96 eV [1]. The high operating temperature of the SOFC source with this electrolyte significantly complicates its technical implementation. Additionally, prolonged operation at high temperature is accompanied by segregation of the dopant atoms leading to the formation of microscopic emissions within the grain boundaries of the electrolyte substance. This causes an increase in the electrical resistance of the electrolyte and, correspondingly, a decrease in the power of the device.

Therefore, there is technological requirement to introduce materials for the SOFC electrolyte that will (i) have high oxygen diffusion (i.e. lower activation energy of diffusion) and (ii) minimum segregation of impurities. Segregation can be limited by using an electrolyte with a minimum content of impurities, and also by lowering the operating temperature. CeO₂ is considered as an intermediate-temperature SOFC (IT-SOFC) electrolyte as it has an electric conductivity coefficient σ in the temperature range 500–1000 °C, which is an order of magnitude larger than YSZ [10–12]. Here we propose to use nano-structured polycrystalline CeO₂ as an IT-SOFC electrolyte because it satisfies these requirements.

Nevertheless, as it is shown in experimental studies, the commonly used coarse-grained (≥ 100 nm) cerium dioxide to a large extent deviates from the stoichiometric

✉ A. Chroneos
ab8104@coventry.ac.uk

¹ Physics Department, V. Karazin Kharkiv National University, Svobody Sq. 4, Kharkiv 61022, Ukraine

² Faculty of Engineering, Environment and Computing, Coventry University, Priory Street, Coventry CV1 5FB, UK

³ Department of Materials, Imperial College London, South Kensington Campus, London SW7 2AZ, UK

composition in this temperature range, especially under conditions of even a small restorative atmosphere. Such a property of the usual size scale CeO_2 crystals leads to the fact that electrons and small-radius polarons (SRP) make an important contribution to the electrical conductivity of this substance. The latter are formed as a result of the interaction of the 4f electrons of Ce^{3+} ions with longitudinal optical vibrations of the crystal lattice [13]. The appearance of Ce^{3+} ions in ceria is due to the changes in its stoichiometric composition (in its chemical formula, CeO_{2-x} , $x > 0$). Naturally, the participation of electrons and polarons in the conductivity of ceria adversely affects its use as an electrolyte for SOFC, since the optimal electrolyte for SOFC must have a sufficiently high conductivity exclusively in relation to oxygen ions.

Here we propose to use stoichiometric cerium dioxide as the contribution of electrons and SRP to the electrical conductivity of this substance is minimal, and the ionic conductivity in the oxygen sublattice is fully realized even in a weakly restorative environment (i.e. air atmosphere). The results indicate that polycrystalline nano structured CeO_2 with a grain size of $\approx (10\text{--}20)$ nm is characterized by more than two orders larger conductivity coefficient σ in comparison to the conductivity of a conventional polycrystal with a grain size $\approx (50\text{--}100)$ nm.

This effect is due to the increase in the oxygen diffusion because of the transport of oxygen ions along the grain boundaries, as well as along the one-dimensional channels formed in the oxygen sublattice of small (nano-sized) crystalline grains. Both diffusion mechanisms are characterized by a much lower activation energy than the activation energy of bulk diffusion in the grains. This motivates the use of this material as an electrolyte for SOFC, operating at temperatures $\approx (300\text{--}600)$ °C, without significant loss of power as compared to SOFC with the YSZ electrolyte. Naturally, a decrease in the temperature range should also help to reduce the “aging” effect of the source, i.e., its degradation during long-term use.

2 Experimental methodology

The studied CeO_2 crystals were synthesized using the “sol–gel” chemical method, in which it is possible to control the size of the crystals by varying the molar ratio of H_2O /surfactant [14]. Crystals of two sizes were used: macro-crystals with a size of $\approx (50\text{--}100)$ nm, and nano-crystals $\approx (10\text{--}20)$ nm. Nano-dimensional crystals were characterized by a special structural state in connection with the manifestation of the so-called “size effect”. Immediately after the preparation, all the crystals were subjected to a stabilizing heat treatment by annealing in an air atmosphere

at a temperature of 1000 °C for 2 h. The average crystal size was determined by electron microscopy.

To measure the electrical conductivity, cylindrical samples with a diameter of 4 mm and a height of 1.5 mm were prepared. Each sample was “compacted” in a special mold at room temperature. The porosity of sample θ was calculated by comparing the sample’s density with the tabulated value of the CeO_2 crystal density. In the following, the porosity value was taken into account to correct the measured value of the electrical conductivity coefficient of the material [15]. In all the samples we studied, $\theta \ll 1$ and, consequently, had practically no effect on the value of the measured specific electrical conductivity of the samples.

To measure the value of the electrical conductivity coefficient σ , the sample was placed in a cell, the body of which was made of an insulator (pyrophyllite), whereas as contacts we used stainless steel rods. The sample temperature during the conductivity measurements was monitored with a copper-constantan thermocouple and varied in the interval (100–600) °C. The measurement of σ was carried out by a standard method using an alternating current with frequency ≈ 1 kHz in air atmosphere.

3 Results and discussion

3.1 Structural state and stoichiometry of CeO_2 nano-crystals

The ratio of the radii of the ions Ce^{4+} and O^{2-} is 0.77, causing the formation of the “fluorite” type lattice [16]. In this lattice Ce^{4+} form a cubic face-centered lattice, while O^{2-} are located in the centers of small cubes, into which the unit cell can be divided. Therefore, each cerium ion is surrounded by eight oxygen ions located at the vertices of the cube, and each oxygen ion is surrounded by four cerium ions located at the vertices of the regular tetrahedron. Such a crystal structure corresponds to the densest packing of cerium and oxygen ions in the (111) planes with coordination (8:4) and at the same time ensures the fulfillment of the electrical neutrality condition of the crystal.

However, the structural state of the CeO_2 crystal described above is characteristic only for the crystals of the usual size scale ≥ 100 nm. With a decrease in crystal size to ≈ 10 nm (nano-crystal), a so-called near-surface structural rearrangement occurs [17]. The reason for such a rearrangement is that for ions located at the surface of the crystal and in a near-surface layer of thickness $\delta \approx 3a$ (a is the parameter of the crystal lattice), the number of the nearest neighbors (the number of ions of the first and subsequent coordination spheres) decreases.

An elementary estimation shows that for a crystal size $d \approx 10$ nm, about half of ions are “sensing” the absence of

the half of the space. The natural consequence of the change in the number of nearest neighbors (change in the coordination number) in nano-crystals is that the “surface” and “near-surface” ions are forced to shift to new positions. Thus, the frequencies of ion oscillations change, their polarization changes and, accordingly, the character of their interaction changes. In ionic compounds of the AB_2 type, the emerging polarization, although significant, is still insufficient for a transition from the “fluorite” structure to some other structure with a different coordination number.

As a rule, there form specific transition structures—the so-called “layered” crystal lattices [16]. As a result of this transformation, symmetry and translational order in the ionic arrangement in the crystals of this class are violated, which ultimately causes a change in the valency of the cations and, correspondingly, a change in the stoichiometry. It is this structural adjustment, i.e. the formation of a “layered” crystal lattice, as well as a change in the stoichiometric composition, occur in CeO_2 crystals with a decrease in their size to ≈ 10 nm. This is supported by the following experimental facts. Firstly, spectral studies have shown that in crystals of this size, the valence of the cation changes, $Ce^{4+} \rightarrow Ce^{3+}$, i.e., there is a transformation of CeO_2 to the sesquioxide Ce_2O_3 [18]. Secondly, due to a change in the valence of the cation, additional (“nonstoichiometric”) vacancies are formed in the anion sublattice of the crystal. Indeed, from the condition of the electric neutrality of the crystal it follows that in the transformation of two Ce^{4+} ions into Ce^{3+} ions, one additional oxygen vacancy forms. Thus, it should be considered that the “layered” lattice in ionic AB_2 type crystals is formed by imposing a series of packets, each of which consists of a layer of cations enclosed between two layers of polarized anions [16].

In the case of CeO_2 nano-crystals, during the formation of a “layered” crystal lattice, each packet is formed from a layer of Ce^{3+} ions (cations) located between two layers of O^{2-} (anions) ions. One such layer is schematically represented in Fig. 1. A peculiarity of this structure is the asymmetric coordination of ions: while the three cations are symmetrically surrounded by six anions located at the apexes of the octahedron, two anions, located in the layer and connected with one cation on one side of it. The polarization of ions due to this structure practically does not change the distance between oppositely charged ions, but the distance between ions of the same sign substantially increases. To preserve the greatest degree of ions’ packing in the (111) planes, rows are formed in them in which ions of the same sign are located. Due to the decrease in the bond energy between the ions in these rows, the formation of “nonstoichiometric” vacancies becomes more likely particularly in the oxygen sublattice. This conclusion was confirmed experimentally [19], in which it was determined that the energy of vacancy formation in the

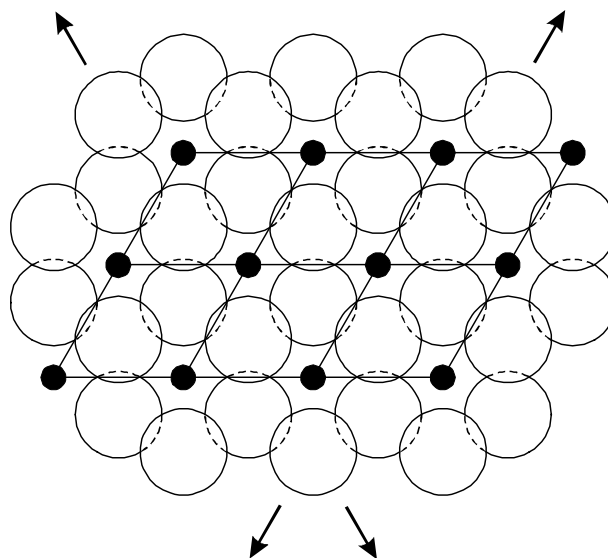


Fig. 1 The crystal structure of a layered lattice. filled circle—Ce; open circle—O

oxygen sublattice of the CeO_2 crystal decreases from 4.5 eV (in the bulk crystal with the “fluorite” lattice) to 0.25 eV (nano-crystal, “layered” lattice).

The process of structural rearrangement occurring in CeO_2 nano-crystals, leads to the formation of ordered clusters (one-dimensional channels) consisting of “nonstoichiometric” oxygen vacancies. Experimentally, the formation of such one-dimensional hollow channels in CeO_2 nano-crystals was detected by high-resolution electron microscopy [20].

To summarize, the structural rearrangement occurring in CeO_2 crystals with a decrease in its size to a value of about 10 nm causes the transformation of the “fluorite” type crystalline lattice into a “layered” type lattice. Such a rearrangement is associated with a “dimensional effect” and is accompanied by a change in the stoichiometry of the crystal, i.e. it is accompanied by a phase transformation $CeO_2 \rightarrow Ce_2O_3$ with simultaneous formation of one-dimensional hollow channels consisting of oxygen vacancies in the anion sublattice of the crystal. Such channels are located in close-packed crystallographic planes (111), oriented along [111] type directions, and can penetrate crystals with a size ≤ 10 nm.

The presence of one-dimensional hollow channels in the anion sublattice of CeO_2 nano crystals causes the accelerated diffusion transport of oxygen ions due to a decrease in the activation energy (the so-called “single-file diffusion” mechanism) [21, 22]. It is this unique structure of nanometer-sized crystals that motivates their use as electrolytes in SOFCs. Additionally, the use of the CeO_2 electrolyte in the form of a nano-structured material with grain size ≈ 10 nm can also contribute to an increase in the oxygen self-diffusion due to their migration along the grain boundaries.

In a polycrystal with such a small grain size, the total area of the boundaries increases significantly, and the diffusion transport of ions along the boundaries is much faster than in the grain volume, since $D_B \gg D_V$ (D_B is the diffusion coefficient in the grain boundary) [23]. A quantitative assessment of the contribution of the two possible ways to enhance the diffusion permeability of oxygen ions in nanostructured polycrystals, follows in the next section.

Notably, in the nano-structured material CeO_2 in the equilibrium state is practically converted to the sesquioxide Ce_2O_3 , i.e., the stoichiometry of this substance changes more. This blocks the formation of polarons, and the small grain size significantly limits the mean free path of the electrons. Thus, the contribution of these undesirable charge carriers to the conductivity of nano-structured CeO_2 is minimized, which also reinforces the use of cerium oxide as an electrolyte in IT-SOFC.

3.2 Intensification of oxygen diffusion in nano-structured CeO_2

This section considers the quantitative evaluation of the degree of intensification of oxygen diffusion in the nano-structured polycrystalline CeO_2 . Firstly, we will estimate the possible contribution in the process of enhancing of the oxygen diffusion in a nano-structured polycrystal due to the increase of the total area of grain boundaries. The transport of a substance in a polycrystalline material taking into account the presence of grain boundaries is characterized by an effective diffusion coefficient

$$D_{\text{ef}} = C_1 D_V + C_2 D_B \delta / d, \quad (2)$$

where D_V and D_B are respectively the diffusion coefficients in the grain volume and in the boundary, δ is the width of the boundary, d is the grain size, C_1 and C_2 are numerical factors [23]. For the quantitative estimation of the possible increase in the oxygen diffusion due to the presence of grain boundaries, we can use the dimensionless ratio: $\chi = D_{\text{ef}} / D_V$. Herewith, it should be taken into account that at temperatures < 500 °C the main process that determines the diffusion transport of matter is the movement of oxygen along the grain boundaries, that is, the first term in Eq. 2 can be neglected, and thus:

$$\chi \approx C_2 D_B \delta / d D_V. \quad (3)$$

Substituting in Eq. 3 reasonable values of: $C_2 \approx 1$, $\delta \approx 1$ nm, $D_B / D_V \approx 10^4$ (at $T \approx 500$ °C), $d \approx 10$ nm, we get: $\chi \approx 10^3$. The evaluation shows that using the nano-structured polycrystalline CeO_2 as an electrolyte for SOFC, it is possible to substantially increase the effective diffusion coefficient of oxygen ions, and, consequently, the electrical conductivity of this material at temperatures ≤ 500 °C. Next, we estimate the possible increase in the oxygen diffusion in CeO_2

nano-crystals in which there exist one-dimensional hollow channels in the anion sublattice. As already indicated, in this case, the transport of oxygen ions can be realized by the single-file diffusion mechanism [21, 22]. This mechanism differs significantly from the classical diffusion mechanism, both, within the volume of the material and along the grain boundaries. The difference is as follows: the classical particle's diffusion mechanism in crystals is based on the model of "random walks" [23].

According to this model, the jumps of particles in the process of their thermal migration occur independently of each other, that is, there is no correlation between them: the succeeding jump of the particle does not depend on what its previous jump was. With such a diffusion mechanism, the radius-vector of the mean displacement of a large number of particles is zero, but the mean-square displacement is different from zero and is described by the Einstein–Smoluchowski relation: $\langle X^2(t) \rangle = 2D_V t$ (t is the diffusion time). The correctness of this conclusion was confirmed by previous experimental and theoretical studies [23].

Notably, under the action of this mechanism, the average value of the diffusion displacement of the particle from its initial position $L_d = (2D_V t)^{1/2}$ is much less than the total distance L that it travels during this time, i.e. $L_d \ll L$. This highlights the low efficiency of matter's transport by the classical diffusion mechanism in the volume of the crystal and explains why the penetration depth of the diffusing particles is so insignificant even at a high temperature and for a sufficiently long annealing times.

In the case of "single-file diffusion", the thermal migration of the moving particles is limited to a one-dimensional hollow channel, along which the particles can move only in one direction, and during the migration process cannot pass each other. The root-mean-square displacement of the particles in this diffusion mechanism is described by the following relation:

$$\langle X^2(t) \rangle = 2Ft^{1/2}. \quad (4)$$

Here F is mobility, a specific parameter characterizing the displacement of diffusing particles in the "single-file" diffusion regime [21]. By itself, the parameter F cannot be used to characterize the efficiency of diffusion. However, if we apply the model of "random walks" to one particle, moving in one direction and not experiencing interaction with other particles (the analog of "single-file diffusion"), then the mean square displacement can approximately be described with the help of this relation:

$$\langle X^2(t) \rangle \approx \lambda \langle X(t) \rangle. \quad (5)$$

Here $\langle X(t) \rangle$ is the average displacement of the moving particle in the one-dimensional channel and λ is the

distance between the moving particles. Assuming that, in analogy with the classical diffusion mechanism, as applied for the “single-file diffusion” the relation describing the average displacement in the form: $\langle X(t) \rangle = (2D_{sf}t)^{1/2}$ is also satisfied and, taking into account Eq. 5: $D_{sf} \approx 2F^2/\lambda^2$. In this relation, the parameter D_{sf} has the dimension of the diffusion coefficient and can characterize the efficiency of the ions’ motion by the “single-file diffusion” mechanism. As before, to give a quantitative estimation of the possible degree of change in the efficiency of matter’s transport by this mechanism, in comparison to the classical diffusion mechanism acting in the volume of the crystal, we form the dimensionless ratio:

$$\chi = D_{sf}/D_V \approx 2F^2/\lambda^2 D_V. \quad (6)$$

Substituting in Eq. 6 reasonable values: $\lambda \approx 1$ nm, $D_V \approx 10^{-11} \text{ m}^2 \text{ s}^{-1}$ (ionic crystals at temperature $T \approx 500$ °C [23]), as well as the mobility value characteristic for nano-dimensional objects $F \approx 10^{-13} \text{ m}^2 \text{ s}^{-1/2}$ [21], we obtain: $\chi \approx 10^3$. Thus, using an electrolyte based on a CeO_2 nano-structured polycrystalline with a grain size of ≈ 10 nm, it is possible to increase oxygen diffusion by three orders of magnitude, and thus to lower the operating temperature of the source to ≤ 600 °C.

3.3 Experimental results

The results of the measurements demonstrated in Figs. 2 and 3, show that the specific electric conductivity for the both types of samples, depends essentially on the temperature and increases exponentially by its increase. The conductivity of the nano-structured sample at a temperature of ≈ 300 °C is more than two orders of magnitude higher than the electrical conductivity of the coarse-grained sample (see Fig. 2). A

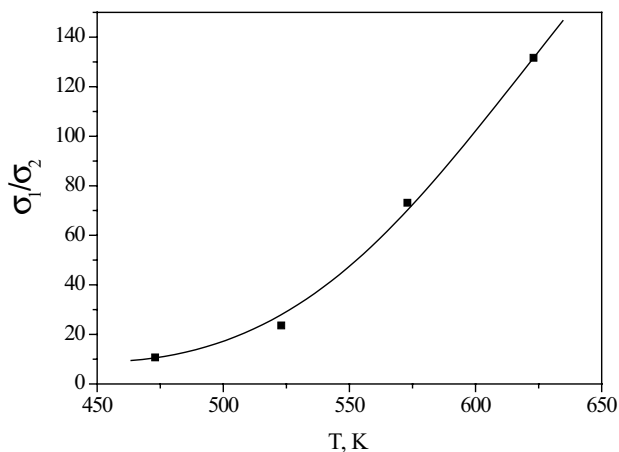


Fig. 2 The temperature dependence of the electrical conductivities ratio of the nano-structured (σ_1) and the coarse-grained (σ_2) polycrystals

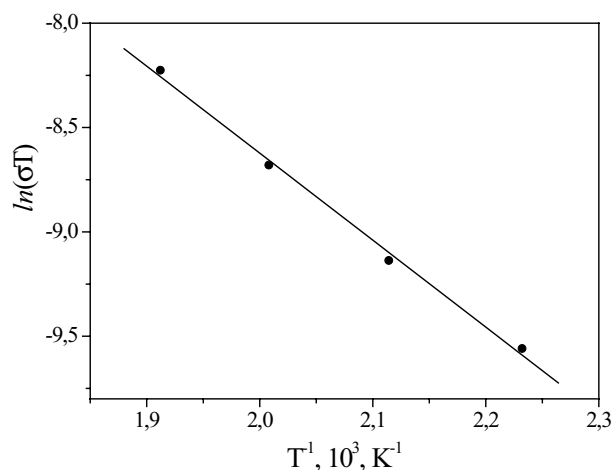


Fig. 3 Temperature dependence of the electrical conductivity of the CeO_2 nano-structured polycrystals

specific role in this may played the specific scattering mechanisms, caused by the existents of structural and kinematic anisotropy in the system [24–26]. The processing of the experimental data in the coordinates $\ln(\sigma T) - 1/T$ indicates a significant decrease in the value of the activation energy Q from ≈ 0.87 eV for the coarse-grained material to ≈ 0.35 eV for the nano-structured polycrystal (refer to Fig. 3). This small value of the activation energy in the case of a nano-structured material is comparable to the energy of formation of oxygen vacancies (≈ 0.25 eV) in CeO_2 nano-crystals, when there are one-dimensional hollow channels present that are formed by the vacancies in the oxygen sublattice [18].

4 Conclusions

It can be concluded that CeO_2 in a nano-structured polycrystalline form is very promising for its use as an electrolyte for IT-SOFC. The experimental data indicates that the most probable factor ensuring an increase in the efficiency of oxygen diffusion is the presence of one-dimensional channels formed by vacancies in the anion sublattice. In this case, in our opinion, the “single-file” diffusion mechanism is realized, that is characterized by a low value of the activation energy of diffusion ≈ 0.35 eV. This constitutes nano-structured polycrystalline CeO_2 a better candidate electrolyte material for IT-SOFC as compared to coarse grained CeO_2 or traditional materials such as YSZ.

Open Access This article is distributed under the terms of the Creative Commons Attribution 4.0 International License (<http://creativecommons.org/licenses/by/4.0/>), which permits unrestricted use, distribution, and reproduction in any medium, provided you give appropriate credit to the original author(s) and the source, provide a link to the Creative Commons license, and indicate if changes were made.

References

1. N. Minh, J. Am. Ceram. Soc. **76**, 563 (1993)
2. S.C. Singhal, Solid State Ionics. **135**, 305 (2000)
3. B.C. Steele, A. Heinzl, Nature **414**, 345 (2001)
4. J. Fleig, Annu. Rev. Mater. Res. **33**, 361 (2003)
5. A.J. Jacobson, Chem. Mater **22**, 660 (2010)
6. J.B. Goodenough, Annu. Rev. Mater. Res. **33**, 91 (2003)
7. A. Tarancón, M. Burriel, J. Santiso, S.J. Skinner, J.A. Kilner, J. Mater. Chem. **20**, 3799 (2010)
8. I.D. Seymour, A. Chroneos, J.A. Kilner, R.W. Grimes, Phys. Chem. Chem. Phys. **13**, 15305 (2011)
9. I.D. Seymour, A. Tarancón, A. Chroneos, D. Parfitt, J.A. Kilner, R.W. Grimes, Solid State Ionics **216**, 41 (2012)
10. M.J.D. Rushton, A. Chroneos, Sci. Rep. **4**, 6068 (2014)
11. R. Blumenthal, F. Brugner, J. Garmier, J. Electrochem. Soc. **120**, 1230 (1973)
12. H. Tuller, A. Nowick, J. Electrochem. Soc. **122**, 255 (1975)
13. V. Ogorodnik, G. Galina, G. Kalnaya, R. Priscepa, Vestnik NTUU, **30**, 82
14. A. Serra, V. Severino, P. Calefi, S. Cicilini, J. Alloys Compd. **323**, 667 (2001)
15. S. David, M. Blaszkiewicz, R. Newnham, J. Am. Ceram. Soc. **73**, 2187 (1990)
16. R. Evans, *Vvedenie v kristallogimiyu* (Goschimizdat, Moskva, 1948), p. 367
17. Yu Petrov, *Fizika malyh chastits* (Nauka, Moskva, 1982), p. 275
18. V. Seminko, P. Maksimchuk, N. Kononets, E. Okrushko, I. Bespalova, A. Masalov, Yu. Malykin, Yu. Boyko, Visnyk HNU, «Fizika» **24**, 20 (2016)
19. N. Skorodumova, S. Simak, B. Lundqvist, I. Abrikosov, B. Johansson, Phys. Rev. Lett. **89**, 601 (2002)
20. F. Esch, S. Fabris, L. Zhou, T. Montini, C. Africh, P. Fomasiero, G. Comelli, R. Rosei, Science **309**, 752 (2005)
21. K. Hahn, J. Karger, V. Kukla, Singl, Phys. Rev. Lett. **76**, 2762 (1996)
22. S. Nedeia, Phys. Rev. E **67**, 1 (2003)
23. B. Bokshtein, S. Bokshtein, A. Zhukhovitskij, *Termodinamika i kinetika diffuzii v tverdyh telah* (Metallurgiya, Moskva, 1974), p. 280
24. P.G. Curran, V.V. Khotkevych, S.J. Bending, A.S. Gibbs, S.L. Lee, A.P. Mackenzie, Phys. Rev. B **84**, 104507 (2011)
25. V.M. Apalkov, M.E. Portnoi, Phys. Rev. B **65**, 125310 (2002)
26. I.N. Adamenko, K. E. Nemchenko, V.I. Tsyganok, A.I. Chervanev, Low Temp. Phys. **20**, 498 (1994)